The EMBO Journal (2006) 25, 2814–2827 | © 2006 European Molecular Biology Organization | All Rights Reserved 0261-4189/06
www.embojournal.org

THE EMBO JOURNAL

Misorientation and reduced stretching of aligned sister kinetochores promote chromosome missegregation in EB1- or APC-depleted cells

VM Draviam[1], I Shapiro[1], B Aldridge[2] and PK Sorger[1,2,*]

[1]Department of Biology, Massachusetts Institute of Technology, Cambridge, MA, USA and [2]Biological Engineering Division, Massachusetts Institute of Technology, Cambridge, MA, USA

The correct formation of stable but dynamic links between chromosomes and spindle microtubules (MTs) is essential for accurate chromosome segregation. However, the molecular mechanisms by which kinetochores bind MTs and checkpoints monitor this binding remain poorly understood. In this paper, we analyze the functions of six kinetochore-bound MT-associated proteins (kMAPs) using RNAi, live-cell microscopy and quantitative image analysis. We find that RNAi-mediated depletion of two kMAPs, the adenomatous polyposis coli protein (APC) and its binding partner, EB1, are unusual in affecting the movement and orientation of paired sister chromatids at the metaphase plate without perturbing kinetochore–MT attachment *per se*. Quantitative analysis shows that misorientation phenotypes in metaphase are uniform across chromatid pairs even though chromosomal loss (CIN) during anaphase is sporadic. However, errors in kinetochore function generated by APC or EB1 depletion are detected poorly if at all by the spindle checkpoint, even though they cause chromosome missegregation. We propose that impaired EB1 or APC function generates lesions invisible to the spindle checkpoint and thereby promotes low levels of CIN expected to fuel aneuploidy and possibly tumorigenesis.

The EMBO Journal (2006) **25,** 2814–2827. doi:10.1038/sj.emboj.7601168; Published online 8 June 2006
Subject Categories: cell cycle
Keywords: aneuploidy; chromosome segregation; kinetochore; microtubule-associated protein

Introduction

Kinetochores are multiprotein structures that assemble on centromeric DNA and mediate the attachment of chromosomes to microtubules (MTs). During metaphase, pairs of sister kinetochores undergo a complex series of movements in which they capture the plus ends of MTs emanating from centrosomes and also nucleate the formation of MTs that are guided toward the poles, so as to form stable bipolar attachments to the mitotic spindle (Kapoor, 2004). Following the completion of bipolar attachment by all chromatid pairs, and the consequent silencing of the Mad- and Bub-dependent spindle checkpoint, sister chromatids disjoin and move towards poles, around which daughter cells form (Musacchio and Hardwick, 2002). In many MT-based processes, motors and MT-associated proteins (MAPs) work together to regulate MT dynamics in a spatially controlled manner and to generate forces necessary for directed movement (Howard and Hyman, 2003). Thus, the establishment of bipolarity is thought to depend on the capture of MTs by kinetochores and the subsequent regulation of MT +end polymer dynamics by MAPs and motors.

A critical question in the study of mitosis is determining why CIN and aneuploidy are more frequent in tumor cells than in normal cells (Lengauer *et al*, 1997). The process of MT capture by kinetochores is stochastic and therefore takes different lengths of time in different cells. The function of the spindle checkpoint is to monitor the capture process in each cell and ensure that anaphase is not initiated until all sister kinetochore pairs are correctly MT-bound. Thus, one possible cause of CIN is that checkpoint pathways are not functional in tumor cells. However, while CIN is observed in yeast carrying mutations in either checkpoint or kinetochore genes (Spencer *et al*, 1990), analogous mutations in human cells cause mitotic catastrophe and cell death (Draviam *et al*, 2004). Thus, it is not surprising that only few human tumors have been found to harbor mutations in Mad and Bub spindle checkpoint genes (Cahill *et al*, 1998; Yamaguchi *et al*, 1999; Sato *et al*, 2000). In contrast to checkpoint and inner kinetochore proteins, outer kinetochore components are attractive as genes whose disruption might impair chromosome–MT attachment while leaving the checkpoint intact (Gergely *et al*, 2003; Meraldi *et al*, 2004; VM Draviam and PK Sorger, unpublished results). Chronic disregulation of kinetochore-bound MAPs (kMAPs) function might have similar effects as low doses of anti-MT drugs such as taxol and the vinca alkaloids, which cause CIN in some cells (Rieder and Maiato, 2004).

Previous work in a variety of eukaryotes has identified many MAPs that localize to kinetochores (Akhmanova and Hoogenraad, 2005). The Dynein–Dynactin motor complex and the + end binding proteins CLIP170 and LIS1 accumulate on kinetochores that are unattached to MTs (Dujardin *et al*, 1998; Faulkner *et al*, 2000). In contrast, EB1 is recruited selectively to kinetochores that are associated with growing MTs (Tirnauer *et al*, 2002) and adenomatous polyposis coli protein (APC), an EB1-binding protein is enriched on kinetochores bound to MTs (Fodde *et al*, 2001; Kaplan *et al*, 2001). Finally, CLASP1 localizes to kinetochores regardless of MT-attachment status (Maiato *et al*, 2003). CLASP1 and CLIP170 regulate kinetochore–MT binding in distinct ways: CLASP1 controls MT dynamics at attached kinetochores (Maiato *et al*,

*Corresponding author. Department of Biology, 68-371 MIT, 77 Mass Avenue, Massachusetts Institute of Technology, Cambridge, MA 02139, USA. Tel.: +1 617 252 1806/1648; Fax: +1 617 253 8550; E-mail: psorger@mit.edu

Received: 21 September 2005; accepted: 4 May 2006; published online: 8 June 2006

2003, 2005), whereas CLIP170 is involved in MT capture (Tanenbaum *et al*, 2006). As expected, depletion of CLIP170 or CLASP1 interferes with bipolar MT binding and causes cells to arrest in mitosis in a checkpoint-dependent manner (Maiato *et al*, 2004; Tanenbaum *et al*, 2006). In the case of Dynein or LIS1, published data are contradictory with respect to function in mitosis and MT binding (Echeverri *et al*, 1996; Faulkner *et al*, 2000; Howell *et al*, 2001; Rogers *et al*, 2002; Green *et al*, 2005). Depletion of the EB1 or APC kMAPs has been reported to cause chromosome misalignment and missegregation (Kaplan *et al*, 2001; Green *et al*, 2005), implying a defect in the checkpoint response, but it is unknown why APC- and EB1-depleted cells divide rather than arrest when misaligned chromosomes are present.

In this paper, we study the effects of disrupting proteins at the kinetochore–MT interface on the generation of CIN in human cells. We use live-cell microscopy and quantitative image analysis to compare directly the fates of mitotic cells that have been depleted of one of six kMAPs by RNAi. We find that depletion of CLIP170, Dynein heavy chain (DHC), LIS1 or chTOG1 prevents normal chromosome congression and results in prolonged checkpoint-dependent mitotic arrest, eventually leading to cell death. In contrast, depletion of EB1 or APC does not significantly interfere with congression, but prevents the formation of an ordered metaphase plate. This leads to sporadic chromosome missegregation at anaphase. The lesions induced by EB1 or APC loss are sensed poorly if at all by the spindle checkpoint, but the checkpoint itself is still functional. We speculate that sporadic missegregation of chromosomes in EB1- or APC-depleted cells represents a type of CIN that might fuel tumorigenesis.

Results

To investigate the effects of depleting kMAPs on kinetochore–MT binding, checkpoint activation and chromosome segregation, we combined RNAi, live-cell microscopy and quantitative image analysis. CLIP170, LIS1, DHC, APC and EB1 were targeted with 4–5 different siRNA oligonucleotides each and the degree of depletion monitored by immunoblotting and immunofluorescence (Supplementary Figure 1; Supplementary Table and data not shown). For each gene, two oligonucleotides resulting in at least 80–90% protein depletion were chosen for further study (Supplementary Table). RNAi-treated HeLa cells ($n \sim 100$ per gene) expressing histone2B (H2B) fused to DsRed were imaged every 3 min for 4–12 h. In each cell, the time of anaphase onset was determined relative to nuclear breakdown (NBD), which was set as $t = 0$. Chromosomes that had not congressed to the metaphase plate prior to anaphase, or that remained away from the metaphase plate for >45 min in arrested cells, were scored as unaligned; those that remained stranded at the spindle equator after anaphase A (chromatid disjunction) were scored as lagging. The fragmentation of chromatin and membrane blebbing (markers of cell death), the orientation of the metaphase plate, elongation of cells in anaphase B and ingression of the furrow during cytokinesis were scored from phase-contrast and fluorescence images.

In control cells ($n = 81$), chromosomes were observed to align at the spindle equator by $t = 20 \pm 1.5$ min, followed 6–8 min later by anaphase (at $t = 26 \pm 2$ min; Meraldi *et al*, 2004). Fewer than 7% of cells had unaligned chromosomes at the time of anaphase onset and no cell death was observed. In contrast, 70–90% cells ($n \sim 100$ per gene) depleted of chTOG1, DHC, CLIP170 or LIS1 remained arrested in mitosis for >3 h without visible cell body elongation or cytokinetic furrow ingression (Figure 1A and B). The severity of the misalignment defect and the precise morphology of the mitotic spindle varied among kMAP depletions (as will be described in detail elsewhere; Supplementary Table), but in all cases, the majority of cells arrested in mitosis had failures of chromosome congression with two or more chromosomes scattered along the spindle axis distant and far from the spindle equator (Figure 1A and C); ~ 90% of cells that remained arrested for >3 h underwent cell death. In chTOG1-, DHC-, CLIP170- or LIS1-depleted cells, high levels of Mad2 and Bub1 were present on misaligned kinetochores for many hours, whereas in control cells, the levels of kinetochore-bound Mad2 and Bub1 fell as prometaphase proceeded (Supplementary Figure 2). To confirm that mitotic arrest provoked by kMAP depletion was checkpoint dependent, cells were codepleted of Mad2. In all cases, >98% of codepleted cells bypassed the checkpoint as evidenced by early anaphase onset (Figure 1D) followed by anaphase B elongation and cleavage furrow ingression. Taken together, these data show that, in the absence of chTOG1, DHC, CLIP170 or LIS1, chromosome congression to the metaphase plate is impaired, a sustained checkpoint signal is generated and cell death ensues.

Mitotic phenotypes of EB1 or APC depletion

The phenotypes associated with EB1 or APC depletion were strikingly different from those of other kMAP depletions. Chromosomes congressed correctly to the spindle equator in most cells and anaphase ensued with little or no delay (Figures 1A and 2A). During anaphase, however, 60–70% of EB1- or APC-depleted cells ($n > 200$ cells) had one or more chromosomes or chromatin strands stranded at spindle equator (Figures 1A and 2B). The appearance of these lagging strands suggested that kinetochores were not bound to MTs in a manner compatible with normal disjunction. Why, then, was the spindle checkpoint not fully activated? One possibility was that EB1 or APC depletion interfered with checkpoint function. To test this, EB1- and APC-depleted cells were treated with nocodazole, an MT-depolymerizing drug, or taxol, an MT-stabilizing drug, and the extent of mitotic arrest evaluated by live and fixed cell imaging (see Figure 2C legend for details). Whereas Mad2 depletion (a positive control) abrogated checkpoint arrest, arrest was efficient and sustained in drug-treated EB1- or APC-depleted cells (Figure 2C). Moreover, immunostaining revealed high levels of kinetochore-bound Mad1, Mad2, Mps1, Bub1 and BubR1 checkpoint proteins in control-, EB1- and APC-depleted prometaphase cells, consistent with an intact checkpoint (Figure 2D; data not shown). Thus, EB1 or APC depletion did not interfere with the operation of the spindle checkpoint.

Despite the similarity between the phenotypes of EB1 or APC depletion, live-cell studies revealed subtle differences in the timing of mitosis. Whereas anaphase timing in EB1-depleted cells ($t = 27 \pm 3$ min, $n = 82$ cells) was indistinguishable from that of control cells ($t = 26 \pm 1$ min, $n = 130$ cells), APC-depleted cells exhibited transient anaphase delay ($t = 85 \pm 9$ min, $n = 70$ cells) (Figure 2A). The differences in anaphase timing were not simply a consequence of differences in the efficiency of RNAi-mediated protein depletion

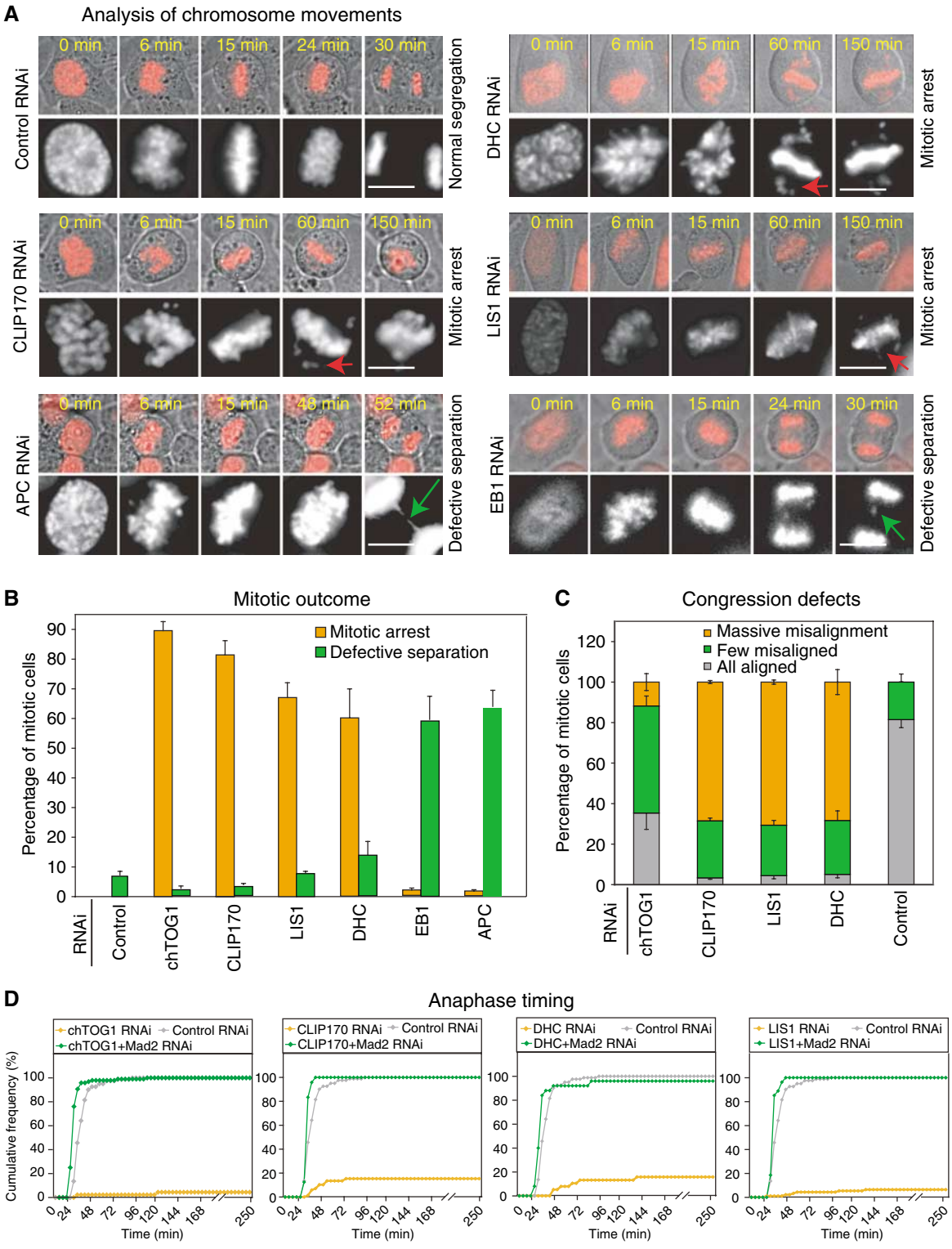

Figure 1 Analysis of mitotic outcome in kMAP-depleted cells. (**A**) Overlay of phase-contrast and fluorescent images of H2B-DsRed-expressing HeLa cells treated with siRNA as indicated. Gray-scale panels are two times magnified fluorescent images of top panels. NBD is set as $t = 0$. Red and green arrows mark uncongressed and lagging chromosomes, respectively. Bar: 10 μm. (**B**) Mitotic outcome in control- or kMAP-depleted cells. Cells were scored as arrested prior to anaphase (orange) or having undergone defective anaphase in the presence of lagging or unaligned chromosomes (green). Error bars show s.d. based on at least three experiments. (**C**) Congression defects in control- or kMAP-depleted cells. Misalignment was visually scored as >5 (massive), 1–5 (few) or no chromosome away from the metaphase plate. (**D**) Cumulative frequency plots of anaphase onset times in siRNA-treated cells as indicated.

since immunofluorescence of individual kinetochores suggests similarly efficient depletion in both cases (Supplementary Figure 3). Anaphase delay caused by APC depletion was abolished by codepletion of Mad2, showing that it reflected checkpoint activation rather than mechanical defects in anaphase spindle elongation. The levels of kinetochore-

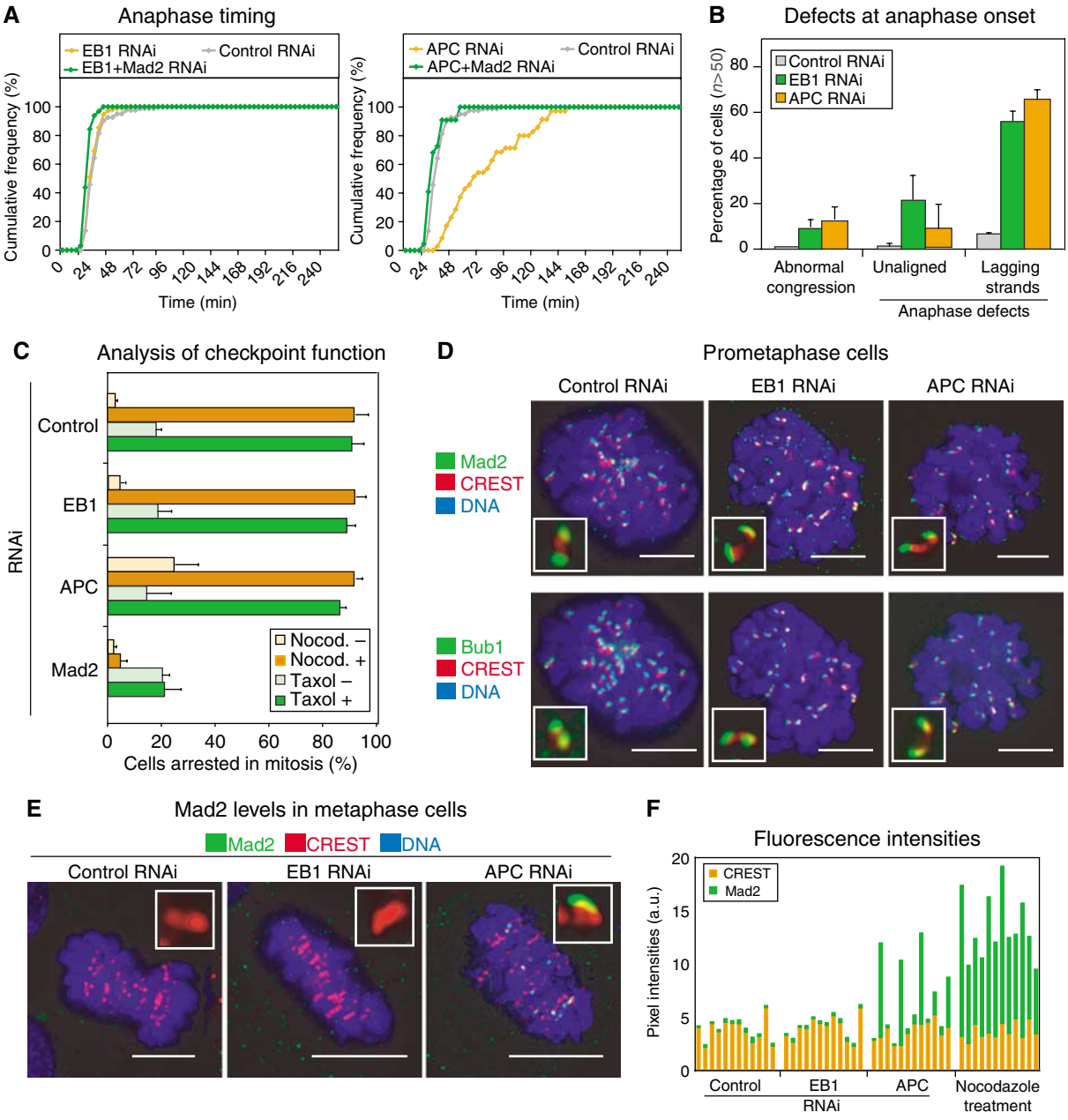

Figure 2 Depletion of EB1 or APC does not abrogate spindle checkpoint response. (**A**) Cumulative frequency plots of anaphase times in siRNA-treated cells as indicated. (**B**) Segregation defects in control-, EB1- or APC-depleted cells. Abnormal congression denotes the presence of unaligned chromosomes 3 min prior to anaphase onset. Cells with anaphase defects were scored as having unaligned chromosomes during anaphase separation or containing lagging chromosomes. Error bars show s.d. based on at least three different experiments. (**C**) Percentage of control-, EB1-, APC- or Mad2-depleted cells arrested in mitosis. In the presence or absence of nocodazole, cells in mitosis for >50 min after NBD were scored as arrested. In the presence or absence of taxol, mitotic arrest was scored by counting DAPI-stained condensed DNA. (**D–E**) Images of prometaphase (D) or metaphase (E) cells treated with siRNA as indicated, and stained with CREST sera to visualize kinetochores (red), and with Mad2 or Bub1 (green) antibodies. (**F**) Fluorescence intensities of Mad2 and CREST signals on kinetochores of siRNA- or nocodazole-treated cells as indicated. Inset: 0.25 × 0.25 μm. Bar: 10 μm.

bound Mad2 on congressed kinetochores in EB1- and control-depleted cells were below the detection limit, but low levels of kinetochore-bound Mad2 were detected on the 4–6 kinetochores per APC-depleted cell delayed in congression to the metaphase plate (Figure 2E and F). Kinetochore-bound Mad2 was lost prior to anaphase in all cells, as expected. Similar but less obvious changes in BubR1 levels were also observed (Supplementary Figure 4). Thus, EB1 depletion resulted in kinetochore–MT attachments that did not maintain a spindle checkpoint-dependant arrest in metaphase, even though lagging chromatids subsequently appeared in anaphase, whereas APC depletion resulted in a more heterogeneous phenotype in which delayed congression of a few chromatid pairs transiently engaged the checkpoint. Importantly, however, the duration of checkpoint-mediated delay in APC-depleted cells was insufficient to allow all defects in kinetochore–MT binding to be corrected and to ensure accurate anaphase disjunction. EB1 and APC depletions were therefore

similar in creating lesions that are not monitored correctly by the spindle checkpoint.

Chromosome missegregation generated by the expression of a dominant-negative EB1 mutant

Next, we tested whether disrupting the interaction between EB1 and APC might phenocopy RNAi in leading to kinetochore defects that failed to engage the spindle checkpoint and thereby caused missegregation in anaphase. EB1 interacts with APC via residues 208–251, and an EB1/1–133 truncation lacking this C-terminal domain associates with MTs but does not bind APC (Figure 3A; Bu and Su, 2003). Overexpression of EB1/1–133-GFP causes a loss of full-length EB1 from MT-tips, but does not affect MT-binding by +end MAPs such as

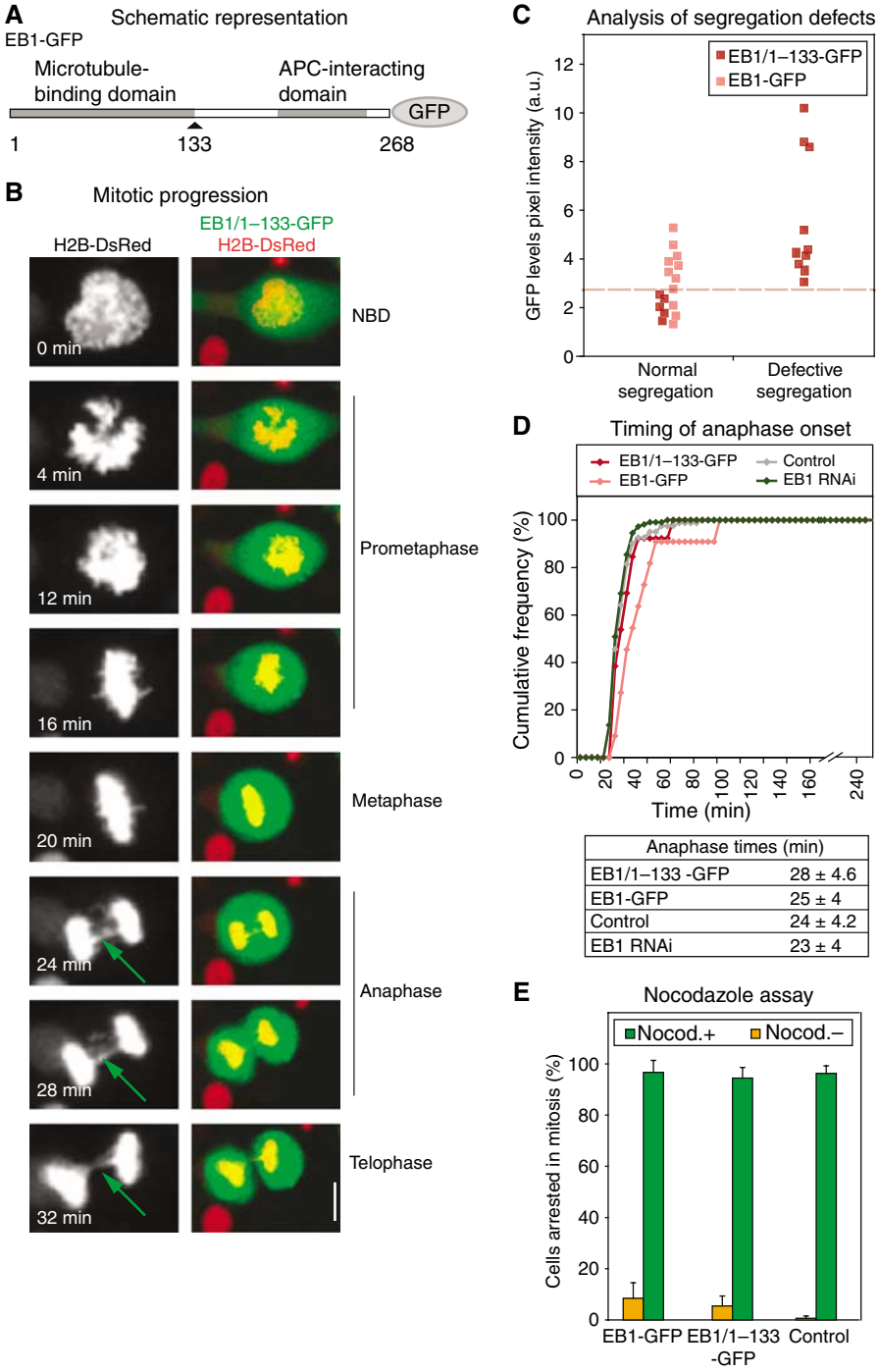

Figure 3 EB1 mutants that cannot bind APC promote missegregation. (**A**) Representation of protein domains in EB1. (**B**) Representative still images of a mitotic cell expressing H2B-DsRed (red) and EB1/1–133-GFP (green). Right panels are overlay and left are gray-scale images intensified and two times magnified. Green arrows mark lagging chromatid strands. (**C**) Plot indicating correlation between expression levels of EB1/1–133-GFP or EB1-GFP (arbitrary intensity units) and missegregation scored as lagging chromosome in anaphase. Dashed line separates high and low expression levels. (**D**) Cumulative frequency plots of anaphase times in cells transfected with siRNA or vectors encoding EB1-GFP or EB1/1–133-GFP as indicated. Table indicates average anaphase times in at least 30 cells. (**E**) Percentage of mitotic cells with or without EB1-GFP or EB1/1-133-GFP expression that remained in mitosis for >50 min after NBD, in the presence or absence of nocodazole. Bar: 10 μm.

CLIP170 (Askham *et al*, 2002; data not shown). To determine whether such a dominant-negative EB1 mutant perturbs mitotic timing and chromosome segregation, H2B-DsRed-expressing HeLa cells were transfected with EB1/1–133-GFP vectors and monitored by live-cell imaging (Figure 3B). Levels of EB1/1–133 expression were estimated on a single-cell basis in the GFP channel and chromosome movement was monitored in the DsRed channel. In all, 75% of transfected cells (18 of 24 cells in three experiments) expressed high levels of EB1/1–133 (>6 a.u.) and all contained lagging chromosomes in anaphase (Figure 3C). In contrast, 100% of control cells (16/16 cells) overexpressing full-length EB1 or cells expressing low levels of EB1/1–133 (<2 a.u.; 5/5 cells) underwent normal segregation (Figure 3C). Anaphase times in these cells were similar to each other and to untransfected control cells (Figure 3D). EB1/1–133 overexpression did not impair the ability of cells to arrest in response to either nocodazole or taxol treatment (Figure 3E; data not shown). From these data, we conclude that expression of a dominant-negative EB1/1–133 protein phenocopies EB1 depletion in that it increases the incidence of lagging chromosomes without engaging the spindle checkpoint or altering the timing of mitosis. Because EB1-associated kMAPs other than APC are not present on kinetochores late in metaphase, we conclude that the binding of APC to EB1 is probably critical for an aspect of chromosome segregation whose disruption cannot be sensed by the spindle checkpoint.

Generation of lagging chromosomes

What defects in kinetochore–MT attachment or spindle structure are responsible for generating lagging chromosomes in EB1- or APC-depleted cells? Based on the roles of EB1 and APC as + end MT-binding proteins, three possibilities suggest themselves: (i) the rate of anaphase chromatid separation might be diminished, increasing the probability that chromosomes lag at the spindle midzone, (ii) kinetochores might not be stably bound to MTs during metaphase and might therefore be left behind during anaphase and (iii) abnormal spindle tumbling induced by the loss of cortical–MT attachments, which are known to require EB1 and APC (Rogers *et al*, 2002; Green and Kaplan, 2003), might interfere with chromatid disjunction. We ruled out possibility (i) by comparing the rates of chromatid separation in control-, EB1- and APC-depleted cells during anaphase A (Supplementary Figure 5). In all three cases, we observed rates similar to those described previously (1.2–1.3 μm/min; Figure 4A; Aist *et al*, 1993). Possibility (ii) was ruled out by examining the effect of cold treatment on kMT stability. Chilling cells prior to fixation destabilizes MTs that are not attached to kinetochores, but has no effect on kMTs (Rieder, 1981). Following 5 min on ice, 3D images of control-, EB1- and APC-depleted spindles were indistinguishable; kinetochores were closely apposed to the + ends of kMT bundles and the kMT bundles were similar in intensity (Figure 4B and Supplementary Figure 6). In contrast, in 3D images of CLIP170-depleted cells, included as a positive control for the cold treatment (Tanenbaum *et al*, 2005), 70% of kinetochores lacked bound MTs or were associated with kinetochore fibers of greatly reduced MT density (Figure 4B and Supplementary Figure 6). We conclude that loss of EB1 and APC does not cause dramatic changes in the extent or stability of MT–kinetochore interactions, in agreement with data showing that checkpoint proteins are not highly enriched on EB1- or APC-depleted kinetochores.

To address the third possibility, that spindle tumbling might interfere with chromatid disjunction, we examined the dynamics of spindle positioning prior to anaphase. EB1 or APC depletion resulted in two spindle positioning defects: displacement of the spindle from the center of the cell and extensive rotation of the spindle axis within the cell (Figure 4C–E; data not shown). The extent of spindle mispositioning varied considerably from cell to cell and we reasoned that the influence of mispositioning on chromatid nondisjunction could be assessed by comparing the degree of displacement and rotation to the number of lagging chromosomes in anaphase. Displacement of metaphase plate was determined from images taken over a 12-min period prior to anaphase onset. Spindle rotation was quantified over the same period by measuring successive solid-angle rotations of the plate. The average displacement of the metaphase plate in EB1- (4.1 ± 1 μm) and APC-depleted cells (6.2 ± 2 μm) was found to be much larger than in control cells (1.7 ± 0.8 μm), and spindle rotation increased three- to five-fold from a modest $18\pm2^\circ$ in control cells to $52\pm4^\circ$ in EB1- and $65\pm2^\circ$ in APC-depleted cells (Figure 4F). However, when displacement and rotation were plotted against lagging chromosome number on a single-cell basis, no correlation was observed: accurate segregation was possible despite dramatic spindle displacement and rotation, whereas segregation errors occurred when displacement and rotation were modest (Figure 4G; data not shown). For example, in EB1-depleted cells, a mean displacement of 3.4 ± 0.8 μm was observed in the absence of lagging chromosomes and 2.2 ± 0.7 μm in the presence of two or more laggards (Figure 4G). We conclude that EB1 and APC are essential for stably positioning spindles, but that spindle mispositioning is not the primary cause of chromosome missegregation in anaphase.

Disordered metaphase plate in EB1- and APC-depleted cells

Although chromosomes congressed to the spindle equator in EB1- or APC-depleted cells, metaphase plates were less compact than in control cells. To quantify the degree of order in the metaphase plate, the rotational angles of k−k axes (line connecting sister kinetochores defining kinetochore orientation) was determined for multiple kinetochores per spindle by examining 3D images of cells expressing the kinetochore marker CENPB-GFP. Typically, 12–18 k−k axes could be distinguished clearly per cell per time point in the 6 min preceding anaphase. The angles describing each set of k−k axes (α_1, β_1, γ_1; α_2, β_2, γ_2; etc.) were then transformed by singular value decomposition (SVD) into a new set of optimal angles (α_1', β_1', γ_1'; α_2', β_2', γ_2'; etc.) and singular values (SVs; σ_1, σ_2, σ_3) (Figure 5A). Under normal circumstances, MTs exert pulling forces on bi-oriented kinetochore pairs causing them to line up in an ordered metaphase with their k−k axis oriented parallel to each other and to the spindle axis (Figure 5B). A set of ordered k−k axes has one high, and two low SVs (Figure 5A, left), whereas a set of disordered axes has more than one high SV (Figure 5A, right). The overall extent of disorder can be captured by the Shannon entropy, which varies from 0, representing perfect order, to 1, representing complete disorder (Figure 5B and see Materials and methods). Importantly, SVD is robust to variability in the

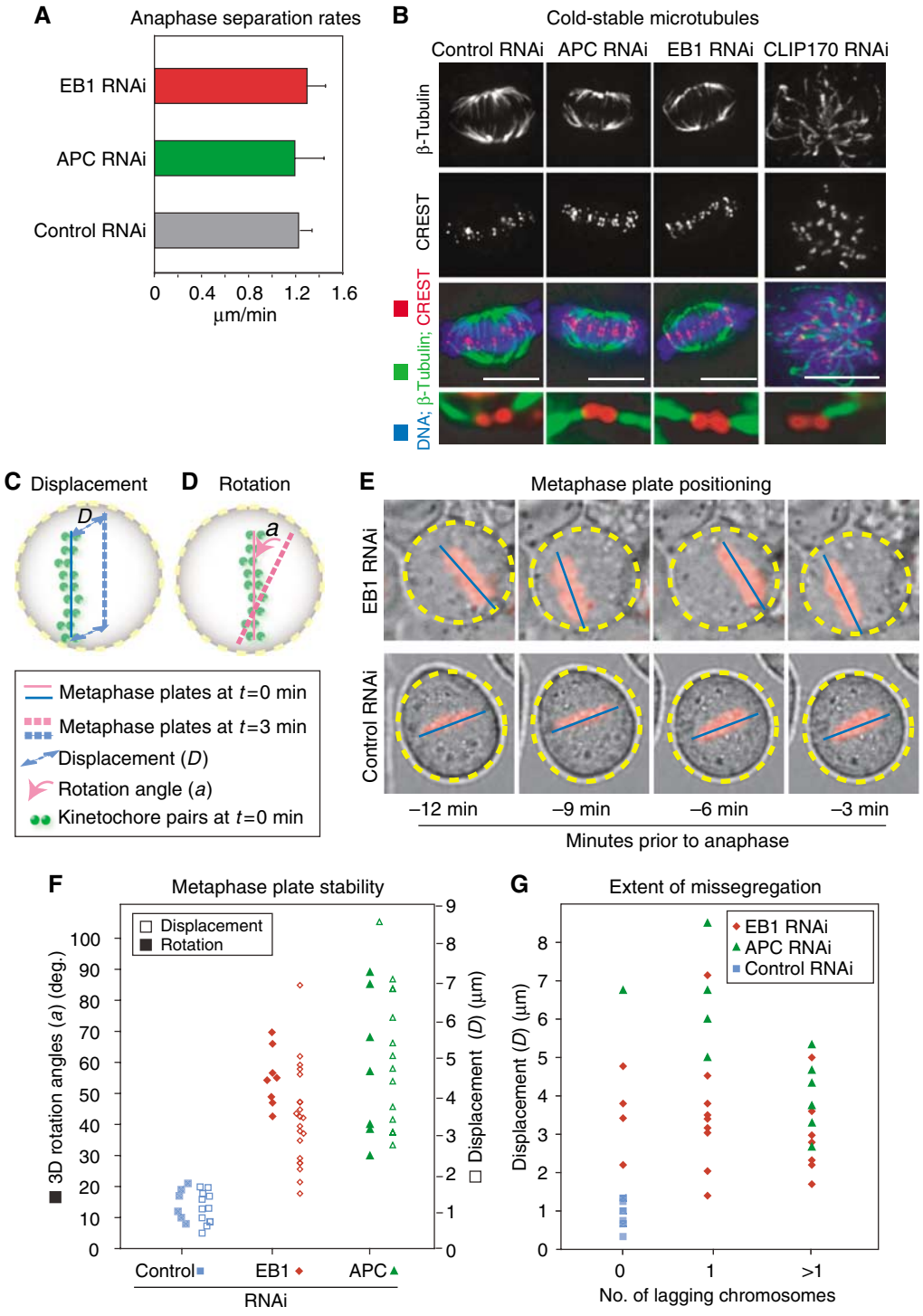

Figure 4 Analysis of lesions in EB1- or APC-depleted cells. (**A**) Average anaphase separation rates in siRNA-treated cells calculated using centroids of anaphase centromeres (see Supplementary Figure 5). (**B**) Images of EB1-, APC-, CLIP170-, or control-siRNA-treated cells costained with β-tubulin antibodies for MTs (green), CREST antisera for kinetochores (red) and DAPI for DNA (blue). Bottom panels are 3D rendered and eight times magnified. (**C, D**) Schematic of metaphase plate positions. Solid and broken lines (pink and blue) indicate the difference between the position of metaphase plate at $t = 0$ and 3 min. (**E**) Overlay of phase-contrast and fluorescent images of metaphase cells treated with EB1- or control-siRNA. Blue lines and yellow circles highlight metaphase plate position with respect to the circumference of the cell. (**F**) Average rotation angles and displacement of metaphase plate every 3 min over a 12-min period prior to anaphase onset in individual cells treated with siRNA as indicated. (**G**) Plot correlating average displacement of metaphase plate and extent of missegregation. Missegregation was scored based on the presence of no lagging strands, or one, or few lagging strands.

number of measurements and is unaffected by large and rapid rotations in the spindle axis, such as those induced by EB1 and APC depletion.

When the Shannon entropy associated with k–k axis orientations was quantified in individual EB1-, APC- or control-depleted cells over a 6-min period prior to anaphase

onset, a striking result was obtained. In control cells, the Shannon entropy started out relatively high (0.68 ± 0.15) but fell rapidly (to 0.03 ± 0.07) 1.5 min before anaphase onset (Figure 5C). In contrast, in EB1- or APC-depleted cells, the Shannon entropy was high throughout the observation period, remaining as high at -1.5 min as at -6 min (0.6–0.7; Figure 5C). In principle, high Shannon entropies might reflect severe misorientation of a few sisters or widespread disorder involving many sisters (Figure 5A). To distinguish between these two extremes we plotted the SVs for individual k–k axes over time. In control cells, only two or three sisters had axes pointing away from the most probable direction by $t = -3$ min (Figure 5D). All of these misorientations were resolved in the minute or two before anaphase onset. In EB1- or APC-depleted cells, in contrast, disorderliness was distributed more or less uniformly across kinetochore pairs and remained high as metaphase proceeded (Figure 5E and F). The difference between control- and APC-depleted cells was highly significant ($P = 0.008$ as estimated using K-Annova) as was the difference between control- and EB1-depleted cells ($P = 0.004$); however, EB1 and APC depletions ($P = 0.87$) were indistinguishable. We therefore conclude that high Shannon entropy in k–k axes in EB1- and APC-depleted cells is due to extensive misorientation involving many sister chromatids.

A second characteristic of metaphase plates observed in EB1- or APC-depleted cells was reduced interkinetochore distance. During metaphase, sister kinetochores are subjected to MT-pulling forces and their extent of separation oscillates between 0.8 and 2.0 μm (Figure 6A; Shelby *et al*, 1996). As expected, when control CENPB-GFP-labeled cells were filmed between $t = -12$ min and -3 min, transient separation was observed, mean interkinetochore distances increased over time and the distribution of distances became more uniform (Figure 6A). Disruption of MT dynamics by brief taxol treatment abolished tension across sister kinetochores; transient separation stopped and interkinetochore distances fell to ~ 1 μm (Figure 6A–C; Kelling *et al*, 2003). In EB1- or APC- depleted cells, brief periods of transient separation were detected, but mean interkinetochore distances were only slightly greater than in taxol-treated cells (Figure 6B and C; Supplementary Figure 7). Like the misorientation of k–k axes, reduced centromere stretching in EB1- or APC-depleted cells was highly penetrant from cell to cell and from one kinetochore pair to the next. Micromanipulation studies have previously established a role for MT-associated pulling forces and tension across kinetochore pairs in metaphase congression (Skibbens *et al*, 1995). Uniformly low level of tension across sisters in EB1- and APC-depleted cells is therefore a likely explanation for the failure of k–k axes to align in parallel at the metaphase plate prior to anaphase onset.

Chromosome missegregation following EB1 and APC depletion

When the Shannon entropy associated with k–k axes was plotted against the number of lagging chromosomes on a cell-to-cell basis, a strong positive correlation was observed (Figure 7A): the greater the entropy, the larger the number of lagging chromosomes. Thus, disorder in the alignment of kinetochore pairs on the metaphase plate was closely associated with chromosome missegregation in anaphase. It was striking, however, that most sister kinetochores were unstretched and misoriented following EB1 or APC depletion, but only a few subsequently missegregated in anaphase. To investigate the relationship between disorder in the metaphase plate and nondisjunction, we attempted to follow individual kinetochore pairs immediately before and after anaphase. In HeLa cells, chromosomes are crowded at the spindle equator and tracking individual kinetochores is technically challenging. However, in four EB1-depleted cells and five APC-depleted cells from four independent experiments, it was possible to trace the kinetochores of lagging chromosomes in anaphase to kinetochore pairs displaying a high degree of k–k axes misorientation late in metaphase (Figure 7B and C). When lagging kinetochores were followed through to telophase, it was also apparent that laggards were incorrectly assorted among daughter cells; unseparated kinetochore pairs were segregated as a set into one daughter cell (Figure 7D). Despite a strong association between metaphase misalignment and lagging kinetochores and between lagging kinetochores and nondisjunction, it is significant that many sister kinetochores with misoriented k–k axes disjoined normally. Thus, EB1 and APC depletion cause highly penetrant problems with orientation and stretching of kinetochore pairs, but a particular kinetochore pair in a single cell still has only a low probability of being missegregated.

Discussion

In this paper, we combine RNAi-mediated protein depletion, live-cell imaging and quantitative analysis to examine the roles of kMAPs on chromosome–MT binding, spindle checkpoint function and CIN. The six kMAPs we have studied share the property that they localize to kinetochores and spindle MTs, but fall into two classes with respect to mitotic depletion phenotypes. Depletion of CLIP170, DHC, LIS1 or chTOG1 perturbs chromosome congression and generates unattached kinetochores that provoke a checkpoint-dependent mitotic arrest. The arrest is sustained and associated with increased cell death, thereby preventing the formation of aneuploid cells. In contrast, following the depletion of EB1 or APC, chromosomes congress to the spindle equator and cells proceed into anaphase with little or no delay. Strikingly, however, these cells missegregate chromosomes. The absence of metaphase arrest in EB1- and APC-depleted cells does not reflect inactivation of the spindle checkpoint, as observed when core kinetochore proteins are depleted (Meraldi *et al*, 2004) since taxol and nocodazole provoke a robust checkpoint response. Instead, lesions created by EB1 depletion appear to be invisible to the checkpoint: they do not lead to checkpoint protein accumulation on kinetochores or to mitotic delay. Lesions created by APC depletion recruit only low levels of Mad2 and provoke only a transient delay (20–30 min) that is insufficient to ensure accurate chromosome segregation. To the best of our knowledge, EB1 and APC are the only kinetochore proteins to date whose depletion phenotypes include defects in metaphase chromosome dynamics that escape checkpoint surveillance and thereby cause sporadic CIN during anaphase. However, it seems likely that other proteins exist with similar loss of function phenotypes, among which we might expect to find tumor suppressor proteins and mutators.

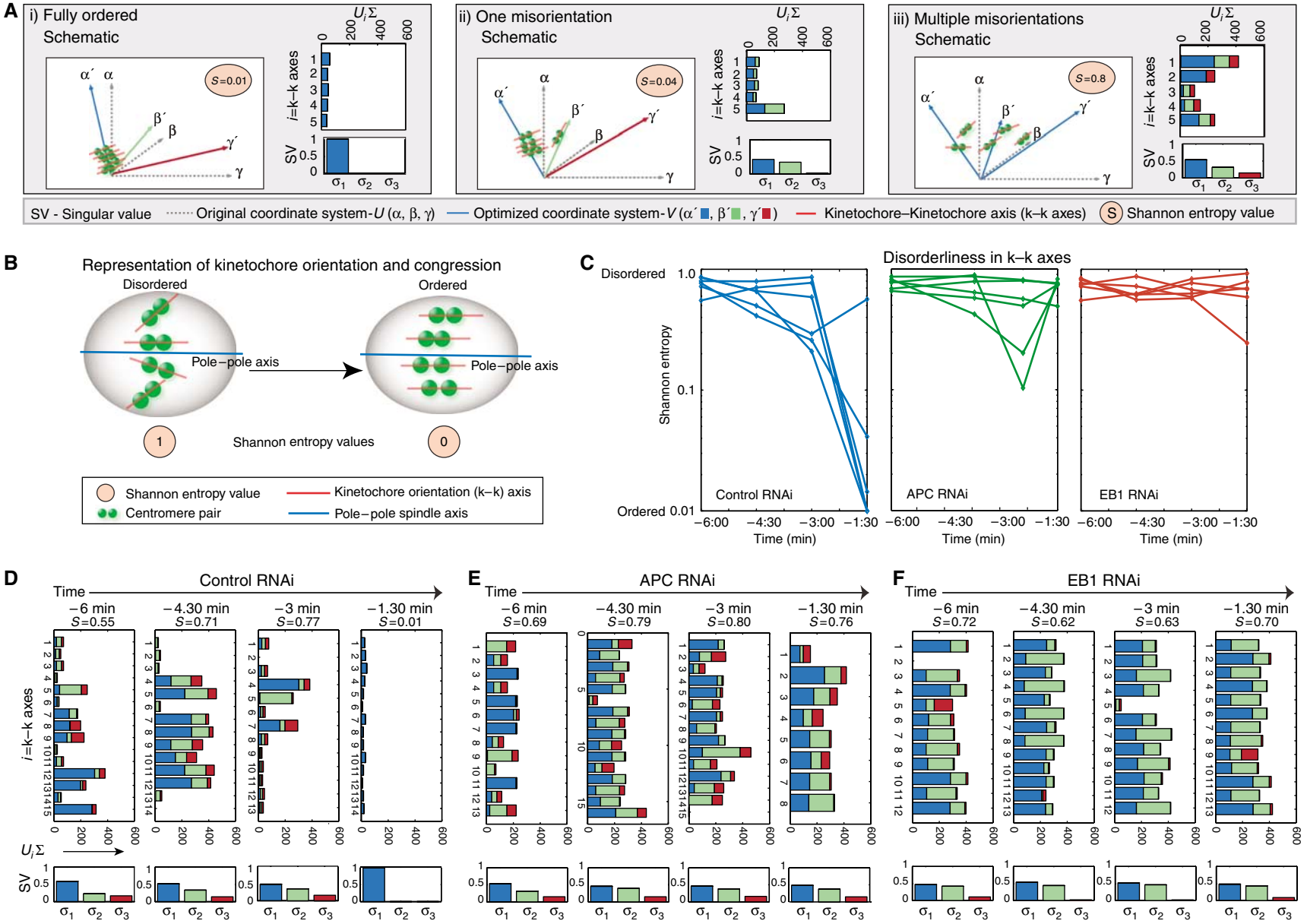

Defects in metaphase plate dynamics caused by EB1 or APC depletion

Although chromosomes in EB1- or APC-depleted cells congressed to the spindle equator, two defects in the resulting metaphase plate were evident: kinetochore pairs did not orient in an orderly manner and they were not fully stretched. In control cells, most kinetochore pairs aligned early in metaphase perpendicular to the spindle equator and oriented parallel to each other. The completion of congression manifested itself as a decrease in the entropy of k–k axis orientations. Concomitantly, interkinetochore stretching increased such that all centromere pairs were stretched by the time anaphase was initiated. The ordered orientation and stretching of centromeres are almost certainly linked: stretching reflects the imposition of pulling forces on pairs of sisters following bi-orientation and causes k–k axes to align parallel to the spindle axis, and thus to each other (Figure 8). In EB1- or APC-depleted cells, in contrast, centromeres do not stretch normally and k–k axes point in different directions. The similarity between EB1 and APC depletion phenotypes sug-

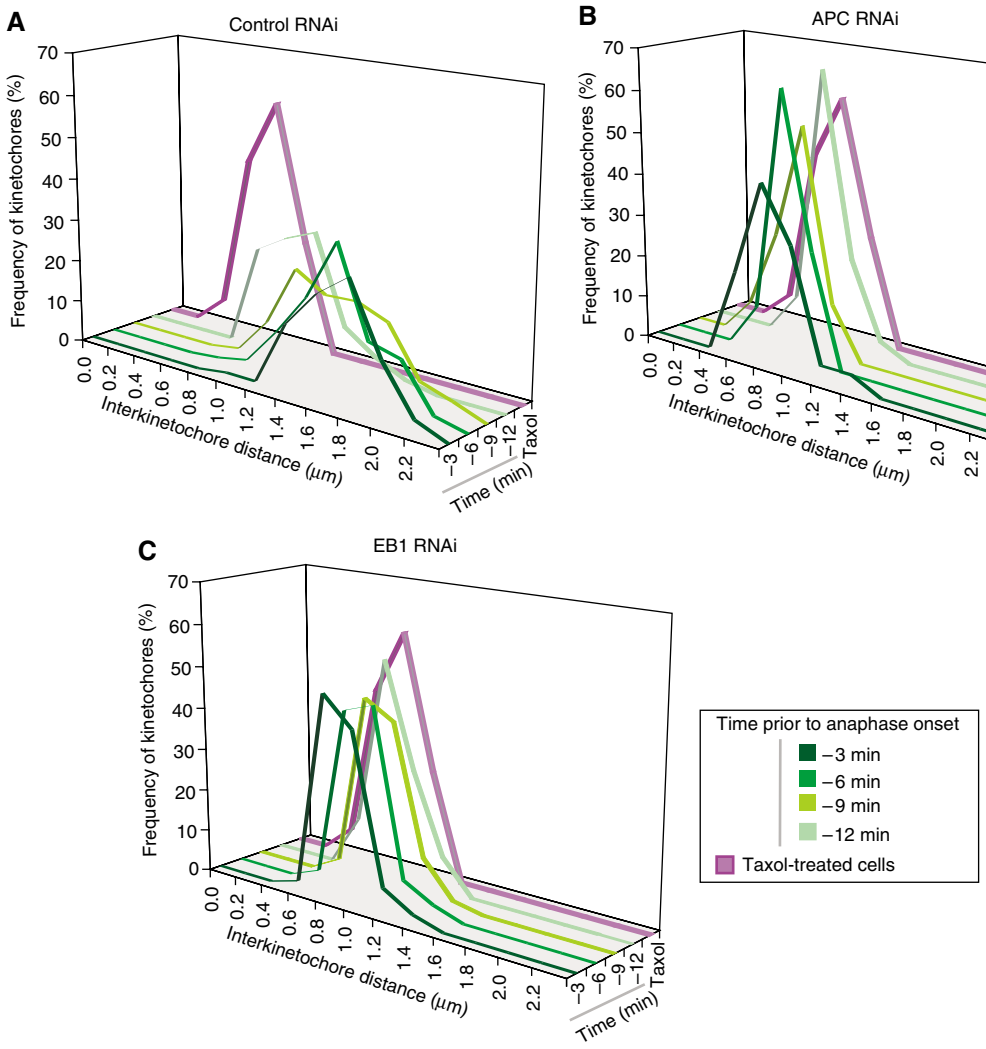

Figure 6 EB1 or APC depletions reduce centromeric stretching. (**A–C**) Frequency distribution of interkinetochore distances in CENPB-GFP-expressing HeLa cells, treated with siRNA against control (A), APC (B) or EB1 (C), calculated from 3D images taken every 3 min for 12-min period prior to anaphase onset. Distances in taxol-treated metaphase cells are plotted in purple. Increasing intensities of green indicate temporal progression.

Figure 5 EB1 or APC depletions perturb orientation of centromeric pairs. (**A**) Schematic representation of three distinct states of k–k axes orderliness. Orthogonal lines indicate orientations of the original coordinate system α, β, γ (gray) and new optimized directions α′, β′, γ′ (blue, green, red). Bar graphs show the contribution of each of the five k–k axes to the optimized directions. Plots below indicate singular values (SV) in three directions (σ_1, σ_2, σ_3). (**B**) Schematic representation of disorderliness in k–k axes of congressed kinetochores. Shannon entropy values for a state of complete disorderliness = 1 and orderliness = 0. (**C**) Shannon entropy of 10–15 k–k axes calculated in each of five cells for a 6-min period prior to anaphase onset. Cells were transfected with control, EB1 or APC siRNA oligos as indicated. (**D–F**) Graphs indicate the contribution of individual k–k axes to optimized direction in cells treated with siRNA against control (D), APC (E) or EB1 (F) calculated from 3D images taken every 90 s for a 6-min period prior to anaphase. Upper panel indicate $U_i\Sigma$ for individual k–k axes. Lower panels indicate SV (σ_1, σ_2, σ_3). *S* indicates Shannon entropy value.

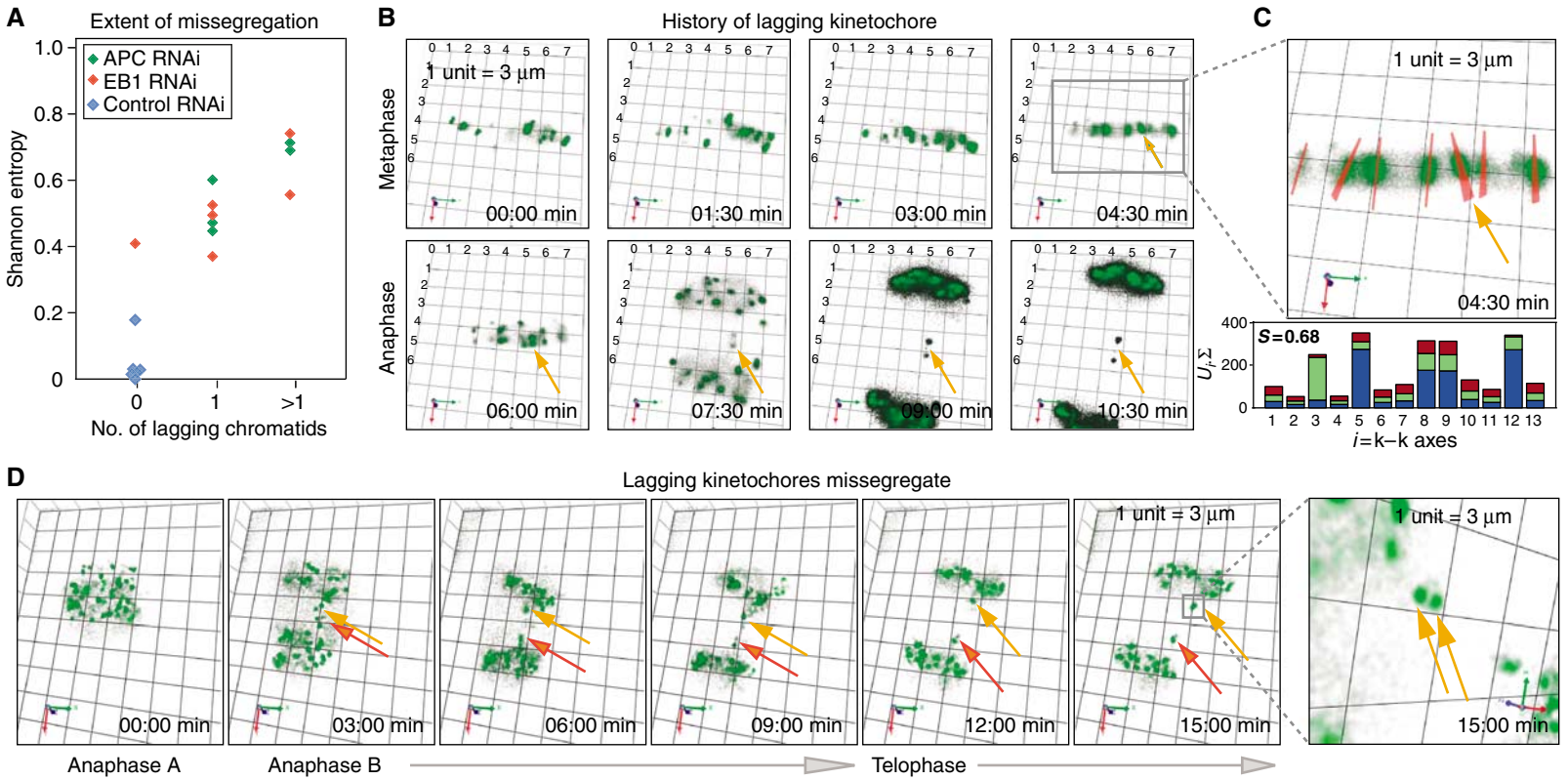

Figure 7 Misoriented centromeres lag in anaphase and undergo missegregation. (**A**) Plot of Shannon entropy values associated with k−k axis orientation in single siRNA-treated cells 90 s prior to anaphase and the number of lagging chromosomes that appeared subsequently in anaphase. (**B**) Rendered images of 5-µm-thick section acquired every 90 s in a CENPB-GFP-expressing cell treated with EB1 siRNA. Orange arrows mark lagging centromeres. (**C**) Three times enlarged image details k−k axes (red) with bold lines projected out of plane and thin lines parallel to plane. Bar graph shows the contribution of individual k−k axes to optimized direction at $t = 4{:}30$ min; S indicates Shannon entropy value. (**D**) Rendered images of 5-µm-thick section acquired every 3 min in a CENPB-GFP-expressing cell treated with EB1 siRNA (orange and red arrows mark lagging kinetochores). Far right panel is 0:6:82 rotated and eight times enlarged; arrows mark unseparated pair. 1 unit = 3 µm.

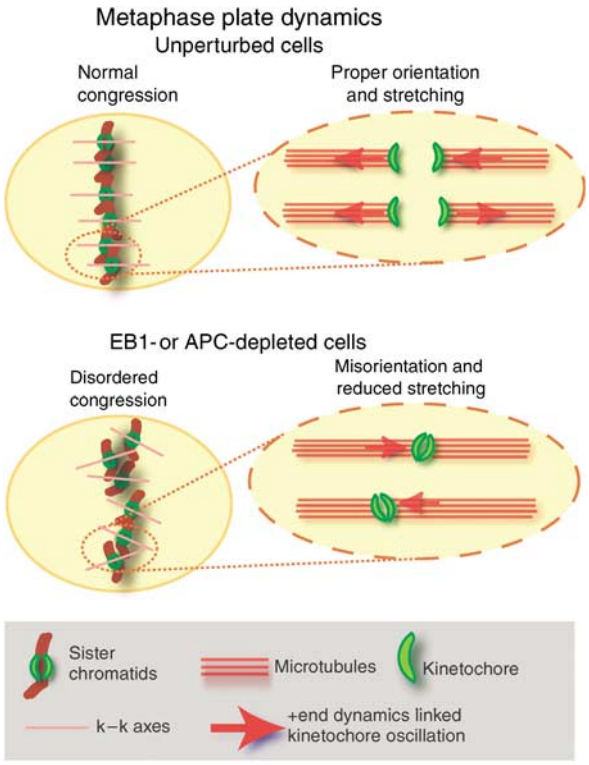

Figure 8 Speculative model for disordered metaphase plate. Schematics show the relationship between ordered congression and kinetochore orientation and stretching. We speculate that in EB1- or APC-depleted cells, the disruption of +end MT dynamics associated with kinetochore oscillations, perturb the orientation and stretching of centromeres.

gests that interaction of the two proteins might be important. EB1 C-terminus contains APC binding site and also the sites for binding to other kMAPs, including p150Glued, CLIP170 and CLASP1. However, p150Glued, CLIP170 leave kinetochores soon after MT-attachment whereas EB1 and APC are present until anaphase (Dujardin *et al*, 1998; Maiato *et al*, 2003; VM Draviam and PK Sorger, unpublished data). EB1 and APC localize in a MT-dependent manner, whereas CLASP1 associates early on with kinetochore in an MT-independent manner (Maiato *et al*, 2003). Thus, anaphase defects observed in cells expressing an EB1 C-terminal deletion mutant probably reflect a dominant-negative effect on APC–EB1 binding.

What prevents kinetochore from becoming stretched and ordered at the metaphase plate in EB1- and APC-depleted cells? One possibility is kMT +end dynamics are disrupted. EB1 is shown to stabilize MT +ends and to accumulate on kinetochores attached to growing MTs (Tirnauer *et al*, 2002). Mutations in APC that disrupt APC–EB1 interaction are reported to increase the frequency of pausing between periods of MT +end growth and shrinkage (Green *et al*, 2005). In EB1- or APC-depleted cells, an increased incidence of +end pausing would perturb the oscillation of sisters along the spindle axis and potentially cause kinetochores to remain unstretched. Reduced stretching would then interfere with the establishment of a preferred k–k orientation (Figure 8). Finally, errors in orientation would give rise to a less compact and staggered metaphase plate, subsequently predisposing cells to missegregation.

Origin of lagging chromatids

One complication in the analysis of MAP loss-of-function phenotypes is that the proteins are typically found at several locations in the spindle. In EB1- or APC-depleted cells, for example, not only is the metaphase plate disordered but spindles undergo rapid tumbling. The extent of tumbling varies from cell to cell, presumably reflecting fluctuations in the MT cytoskeleton. The extent of tumbling is not correlated with the number of lagging chromosomes, however. Many cells segregate chromosomes accurately despite severe tumbling. In contrast, a high level of entropy in k–k axis orientation is strongly correlated with the appearance of lagging chromosomes. Thus, the defects in centromere orientation are linked to nondisjunction, but spindle tumbling is not.

Why does kinetochore misorientation and/or reduced stretching cause chromosome missegregation? We can rule out the possibility that kinetochores fail to achieve bipolar attachment: Mad and Bub protein levels on EB1- or APC-depleted kinetochores are not high, as expected of unattached kinetochores. Alternatively, misorientation might increase the probability that a single kinetochore attaches to MTs emanating from both poles, a state known as merotelic attachment (Cimini *et al*, 2001). By light microscopy, however, merotelic configurations in EB1- or APC- depleted cells are no more frequent than in unperturbed cells (~2%). Although our data do not completely rule out merotely as a cause for missegregation in APC- or EB1-depleted cells, they strongly argue against it. A third possible cause of missegregation is that reduced kinetochore stretching interferes with the formation of specialized cohesion domains around centromeres and therefore interferes with efficient scission of sister–sister links. Consistent with this idea, we frequently observe lagging kinetochores moving as a pair into one of the two daughters before separating and disjoining. A final possibility is that a defect in the local control of kMT shrinkage (as seen in XKCM1 depletion; Kinoshita *et al*, 2006). Distinguishing among these possibilities is difficult, given the relatively low frequency of missegregation events, and all may be involved. For the current discussion, however, the critical point is that a uniform metaphase misorientation phenotype generated by EB1 or APC depletion greatly increases the probability of subsequent problems in anaphase, while nonetheless allowing most chromosomes to segregate normally. The role of EB1 in maintaining a stable genome appears to be conserved through evolution: inactivation of the EB1 homologues Bim1p in *Saccharomyces cerevisiae* or Mal3 in *Schizosaccharomyces pombe* causes CIN (Beinhauer *et al*, 1997; Mayer *et al*, 2004). However, unlike EB1 depletion, Mal3 deletion induces a Bub1-dependent mitotic delay (Asakawa *et al*, 2005).

Implications for checkpoint control

Why are the defects generated by EB1 depletion invisible to the checkpoint and those generated by APC depletion only weakly sensed? Lesions associated with EB1 or APC loss might not involve problems with kinetochore–MT attachment *per se*. This possibility is consistent with our finding that MTs remain kinetochore-bound in cold-treated EB1- or APC-depleted cells and that Mad2 is largely absent from kinetochores by late metaphase. Although Green *et al* (2005) report high numbers of uncongressed chromosomes in APC-

depleted cells, based on a fixed cell assay, our live analysis reveals that APC depletion only delays congression (by 20–40 min), and that this delay is checkpoint dependent. Subsequent misorientation of k–k axes on the metaphase plate is not sensed by the checkpoint. It has been suggested that the absence of tension at kinetochores is itself an inducer of checkpoint arrest, although considerable controversy surrounds this idea (Pinsky and Biggins, 2005). Does the failure of relaxed kinetochore pairs to trigger checkpoint arrest in EB1-depleted cells argue against the hypothesis that tension is monitored? Perhaps, but whereas mean interkinetochore distances are low in both EB1-depleted (checkpoint off) and taxol-treated (checkpoint on) cells, live-cell imaging reveals brief periods of transient separation in the former (Supplementary Figure 7). These brief separations may be sufficient to silence tension-sensitive checkpoint pathways.

We and others have previously demonstrated the existence of four phenotypes associated with the inactivation of checkpoint or kinetochore proteins: (i) RNAi of Mad1 and Bub3 abolishes the checkpoint without altering the timing of mitosis and therefore represents a classic checkpoint lesion, (ii) RNAi of Mad2 and BubR1 inactivates the checkpoint and accelerates the timing of mitosis reflecting an off-kinetochore function for these proteins, (iii) RNAi of Bub1 and AuroraB inactivates the checkpoint and also disrupts normal chromosome congression, implying a role in kinetochore–MT interaction and (iv) RNAi of inner kinetochore proteins interferes with MT attachment and also causes checkpoint inactivation, apparently by preventing kinetochore recruitment of checkpoint proteins (Lens and Medema, 2003; Meraldi *et al*, 2004; Meraldi and Sorger, 2005). The data in this paper add a fifth class: MAPs whose depletion leads to lesions in kinetochore–MT interaction that cannot be sensed by the checkpoint, but nonetheless cause CIN.

CIN and the stochastic nature of nondisjunction

Human tumors are often highly aneuploid, but only a few have been found to harbor mutations in spindle checkpoint genes (Yamaguchi *et al*, 1999; Sato *et al*, 2000; Draviam *et al*, 2004). Perhaps this is to be expected, since loss-of-function checkpoint mutations cause mitotic catastrophe in animal cells and trigger p53-dependent apoptosis (Burds *et al*, 2005). In contrast, while EB1 and APC inactivation generates uniform defects in sister chromatid orientation, only sporadic chromosome loss ensues. Sporadic CIN seems much more likely to promote tumorigenesis than gross errors in mitosis. APC is a tumor suppressor mutated in colorectal cancers, and EB1 also is altered in some tumors (Kinzler and Vogelstein, 1996; Suarez-Merino *et al*, 2005), but it has not been possible to link CIN and tumorigenesis through mutation of APC (Bienz, 2002), in part because APC also plays a critical role in regulating cell proliferation. Additional study of EB1 and APC in mitosis and the generation of separation of function alleles might ascertain whether mitotic errors contribute to cancer. The data in this paper also suggest that it will be highly worthwhile to identify kinetochore proteins other than EB1 and APC whose disruption causes lesions that are invisible to the spindle checkpoint and might therefore promote CIN.

Materials and methods

Live-cell imaging

Cells were imaged using $\times 20$ NA0.75 objective as described in Meraldi *et al* (2004). To image centromere dynamics, $\times 100$ NA1.4 objective equipped with a heater was used.

Cell culture

Vectors encoding H2B-DsRed or CENPB-GFP cDNA were transfected using *Fugene6* and cells were sorted using FACS. For EB1 mutant expression, EB1 cDNA (1–399 bp) was subcloned into pEGFP-N1. Cells were synchronized using thymidine (20 mM; 18 h) and nocodazole (40 ng/ml) was added 10 min prior to imaging. Taxol (40 nM) was added 10 h after thymidine wash and mitotic cells were scored 6 h later.

Quantification of k–k axes disorderliness

Rotation angles (α, β, γ) of k–k axes were obtained from each cell at discrete times using SoftWorx. Sets of angles for n k–k axes were arranged into matrix A ($n \times 3$). svd function in MATLAB was used to compute SVD of $A = U\sum V^T$ where U and V are orthogonal and $\sum$ is diagonal matrix of singular values (σ_1, σ_2, σ_3). SV describes the degree of variation in the angles along each direction in V (α', β', γ'). Shannon entropy of the SV (Alter *et al*, 2000)

$$S = \frac{-1}{\log(L)} \sum_{i=1}^{3} p_i \log(p_i)$$

where

$$p_i = \frac{\sigma_i^2}{\sum_{j=1}^{3} \sigma_j^2}$$

Supplementary data

Supplementary data are available at *The EMBO Journal* Online.

Acknowledgements

We thank S Taylor, W Earnshaw, Y Mimori-Kiyosue, T Schroer, T Hyman and K Sullivan for reagents and members of the Sorger lab for helpful discussion. This work was supported by NIH Grants CA08417 and GM51464.

References

Aist JR, Liang H, Berns MW (1993) Astral and spindle forces in PtK2 cells during anaphase B: a laser microbeam study. *J Cell Sci* **104** (Part 4)**:** 1207–1216

Akhmanova A, Hoogenraad CC (2005) Microtubule plus-end-tracking proteins: mechanisms and functions. *Curr Opin Cell Biol* **17:** 47–54

Alter O, Brown PO, Botstein D (2000) Singular value decomposition for genome-wide expression data processing and modeling. *Proc Natl Acad Sci USA* **97:** 10101–10106

Asakawa K, Toya M, Sato M, Kanai M, Kume K, Goshima T, Garcia MA, Hirata D, Toda T (2005) Mal3, the fission yeast EB1 homologue, cooperates with Bub1 spindle checkpoint to prevent monopolar attachment. *EMBO Rep* **6:** 1194–1200

Askham JM, Vaughan KT, Goodson HV, Morrison EE (2002) Evidence that an interaction between EB1 and p150(Glued) is required for the formation and maintenance of a radial microtubule array anchored at the centrosome. *Mol Biol Cell* **13:** 3627–3645

Beinhauer JD, Hagan IM, Hegemann JH, Fleig U (1997) Mal3, the fission yeast homologue of the human APC-interacting protein EB-1 is required for microtubule integrity and the maintenance of cell form. *J Cell Biol* **139:** 717–728

Bienz M (2002) The subcellular destinations of APC proteins. *Nat Rev Mol Cell Biol* **3:** 328–338

Bu W, Su LK (2003) Characterization of functional domains of human EB1 family proteins. *J Biol Chem* **278:** 49721–49731

Burds AA, Lutum AS, Sorger PK (2005) Generating chromosome instability through the simultaneous deletion of Mad2 and p53. *Proc Natl Acad Sci USA* **102:** 11296–11301

Cahill DP, Lengauer C, Yu J, Riggins GJ, Willson JK, Markowitz SD, Kinzler KW, Vogelstein B (1998) Mutations of mitotic checkpoint genes in human cancers. *Nature* **392:** 300–303

Cimini D, Howell B, Maddox P, Khodjakov A, Degrassi F, Salmon ED (2001) Merotelic kinetochore orientation is a major mechanism of aneuploidy in mitotic mammalian tissue cells. *J Cell Biol* **153:** 517–527

Draviam VM, Xie S, Sorger PK (2004) Chromosome segregation and genomic stability. *Curr Opin Genet Dev* **14:** 120–125

Dujardin D, Wacker UI, Moreau A, Schroer TA, Rickard JE, De Mey JR (1998) Evidence for a role of CLIP-170 in the establishment of metaphase chromosome alignment. *J Cell Biol* **141:** 849–862

Echeverri CJ, Paschal BM, Vaughan KT, Vallee RB (1996) Molecular characterization of the 50-kD subunit of dynactin reveals function for the complex in chromosome alignment and spindle organization during mitosis. *J Cell Biol* **132:** 617–633

Faulkner NE, Dujardin DL, Tai CY, Vaughan KT, O'Connell CB, Wang Y, Vallee RB (2000) A role for the lissencephaly gene LIS1 in mitosis and cytoplasmic dynein function. *Nat Cell Biol* **2:** 784–791

Fodde R, Kuipers J, Rosenberg C, Smits R, Kielman M, Gaspar C, van Es JH, Breukel C, Wiegant J, Giles RH, Clevers H (2001) Mutations in the APC tumour suppressor gene cause chromosomal instability. *Nat Cell Biol* **3:** 433–438

Gergely F, Draviam VM, Raff JW (2003) The ch-TOG/XMAP215 protein is essential for spindle pole organization in human somatic cells. *Genes Dev* **17:** 336–341

Green RA, Kaplan KB (2003) Chromosome instability in colorectal tumor cells is associated with defects in microtubule plus-end attachments caused by a dominant mutation in APC. *J Cell Biol* **163:** 949–961

Green RA, Wollman R, Kaplan KB (2005) APC and EB1 function together in mitosis to regulate spindle dynamics and chromosome alignment. *Mol Biol Cell* **16:** 4609–4622

Howard J, Hyman AA (2003) Dynamics and mechanics of the microtubule plus end. *Nature* **422:** 753–758

Howell BJ, McEwen BF, Canman JC, Hoffman DB, Farrar EM, Rieder CL, Salmon ED (2001) Cytoplasmic dynein/dynactin drives kinetochore protein transport to the spindle poles and has a role in mitotic spindle checkpoint inactivation. *J Cell Biol* **155:** 1159–1172

Kaplan KB, Burds AA, Swedlow JR, Bekir SS, Sorger PK, Nathke IS (2001) A role for the adenomatous polyposis coli protein in chromosome segregation. *Nat Cell Biol* **3:** 429–432

Kapoor TM (2004) Chromosome segregation: correcting improper attachment. *Curr Biol* **14:** R1011–R1013

Kelling J, Sullivan K, Wilson L, Jordan MA (2003) Suppression of centromere dynamics by Taxol in living osteosarcoma cells. *Cancer Res* **63:** 2794–2801

Kinoshita K, Noetzel TL, Arnal I, Drechsel DN, Hyman AA (2006) Global and local control of microtubule destabilization promoted by a catastrophe kinesin MCAK/XKCM1. *J Muscle Res Cell Motil* **27:** 107–114

Kinzler KW, Vogelstein B (1996) Lessons from hereditary colorectal cancer. *Cell* **87:** 159–170

Lengauer C, Kinzler KW, Vogelstein B (1997) Genetic instability in colorectal cancers. *Nature* **386:** 623–627

Lens SM, Medema RH (2003) The survivin/Aurora B complex: its role in coordinating tension and attachment. *Cell Cycle* **2:** 507–510

Maiato H, Fairley EA, Rieder CL, Swedlow JR, Sunkel CE, Earnshaw WC (2003) Human CLASP1 is an outer kinetochore component that regulates spindle microtubule dynamics. *Cell* **113:** 891–904

Maiato H, Khodjakov A, Rieder CL (2005) *Drosophila* CLASP is required for the incorporation of microtubule subunits into fluxing kinetochore fibres. *Nat Cell Biol* **7:** 42–47

Maiato H, Rieder CL, Khodjakov A (2004) Kinetochore-driven formation of kinetochore fibers contributes to spindle assembly during animal mitosis. *J Cell Biol* **167:** 831–840

Mayer ML, Pot I, Chang M, Xu H, Aneliunas V, Kwok T, Newitt R, Aebersold R, Boone C, Brown GW, Hieter P (2004) Identification of protein complexes required for efficient sister chromatid cohesion. *Mol Biol Cell* **15:** 1736–1745

Meraldi P, Draviam VM, Sorger PK (2004) Timing and checkpoints in the regulation of mitotic progression. *Dev Cell* **7:** 45–60

Meraldi P, Sorger PK (2005) A dual role for Bub1 in the spindle checkpoint and chromosome congression. *EMBO J* **24:** 1621–1633

Musacchio A, Hardwick KG (2002) The spindle checkpoint: structural insights into dynamic signalling. *Nat Rev Mol Cell Biol* **3:** 731–741

Pinsky BA, Biggins S (2005) The spindle checkpoint: tension versus attachment. *Trends Cell Biol* **15:** 486–493

Rieder CL (1981) The structure of the cold-stable kinetochore fiber in metaphase PtK1 cells. *Chromosoma* **84:** 145–158

Rieder CL, Maiato H (2004) Stuck in division or passing through: what happens when cells cannot satisfy the spindle assembly checkpoint. *Dev Cell* **7:** 637–651

Rogers SL, Rogers GC, Sharp DJ, Vale RD (2002) *Drosophila* EB1 is important for proper assembly, dynamics, and positioning of the mitotic spindle. *J Cell Biol* **158:** 873–884

Sato M, Sekido Y, Horio Y, Takahashi M, Saito H, Minna JD, Shimokata K, Hasegawa Y (2000) Infrequent mutation of the hBUB1 and hBUBR1 genes in human lung cancer. *Jpn J Cancer Res* **91:** 504–509

Shelby RD, Hahn KM, Sullivan KF (1996) Dynamic elastic behavior of alpha-satellite DNA domains visualized *in situ* in living human cells. *J Cell Biol* **135:** 545–557

Skibbens RV, Rieder CL, Salmon ED (1995) Kinetochore motility after severing between sister centromeres using laser microsurgery: evidence that kinetochore directional instability and position is regulated by tension. *J Cell Sci* **108** (Part 7)**:** 2537–2548

Spencer F, Gerring SL, Connelly C, Hieter P (1990) Mitotic chromosome transmission fidelity mutants in *Saccharomyces cerevisiae*. *Genetics* **124:** 237–249

Suarez-Merino B, Hubank M, Revesz T, Harkness W, Hayward R, Thompson D, Darling JL, Thomas DG, Warr TJ (2005) Microarray analysis of pediatric ependymoma identifies a cluster of 112 candidate genes including four transcripts at 22q12.1–q13.3. *Neuro-oncology* **7:** 20–31

Tanenbaum ME, Galjart N, van Vugt MA, Medema RH (2005) CLIP-170 facilitates the formation of kinetochore–microtubule attachments. *EMBO J* **25:** 45–57

Tanenbaum ME, Galjart N, van Vugt MA, Medema RH (2006) CLIP-170 facilitates the formation of kinetochore–microtubule attachments. *EMBO J* **25:** 45–57

Tirnauer JS, Canman JC, Salmon ED, Mitchison TJ (2002) EB1 targets to kinetochores with attached, polymerizing microtubules. *Mol Biol Cell* **13:** 4308–4316

Yamaguchi K, Okami K, Hibi K, Wehage SL, Jen J, Sidransky D (1999) Mutation analysis of hBUB1 in aneuploid HNSCC and lung cancer cell lines. *Cancer Lett* **139:** 183–187